Update of joint CPUE indices for the bigeye tuna in the Indian Ocean based on Japanese, Korean and Taiwanese longline fisheries data up to 2021

Toshihide Kitakado[1], Sheng-Ping Wang[2], Takayuki Matsumoto[3], Sung Il Lee[4], Keisuke Satoh[3], Hiroki Yokoi[3], Kei Okamoto[3], Mi Kyung Lee[5], Jung-Hyun Lim[5], Youjung Kwon[5], Wen-Pei Tsai[6], Nan-Jay Su[2], Su-Ting Chang[7] and Feng-Chen Chang[7]

[1] Tokyo University of Marine Science and Technology, 5-7, Konan 4, Minato, Tokyo, 108-8477, Japan (Email: kitakado@kaiyodai.ac.jp)

[2] National Taiwan Ocean University, No. 2, Beining Rd., Zhongzheng Dist., Keelung City 20224, Taiwan

[3] National Research and Development Agency, Japan Fisheries Research and Education Agency, Fisheries Resources Institute, 2-12-4 Fukuura, Kanazawa-ku, Yokohama-shi, kanagawa-ken, 236-8648, Japan

[4] Pukyong National University, 45 Yongso-ro, Nam-gu, Busan 48513, Korea

[5] National Institute of Fisheries Science, 216 Gijanghaean-ro, Gijang-eup, Gijang-gun, 46083 Busan, Korea

[6] National Kaohsiung University of Science and Technology, No. 415, Jiangong Rd., Sanmin Dist., Kaohsiung City 80778, Taiwan

[7] Overseas Fisheries Development Council, 3F., No.14, Wenzhou St., Da'an Dist., Taipei City 10648, Taiwan

ABSTRACT

Joint CPUE standardization was conducted for the Indian Ocean bigeye tuna based on Japanese, Korean and Taiwanese longline fisheries data up to 2021 to provide the WPTT with information on abundance indices for use in the 2021 stock assessment for this stock. The intention was to produce combined indices by increasing the spatial and temporal coverage of fishery data. Due to the limitation of remote access to the data, an approach adopted among the three members for the previous analyses of tropical tunas for IOTC and ICCAT was used to share only aggregated data. To account for the inter-annual changes of the target in each fishery, information on the HBF or clustering result was used in each region. For standardizing the catch-per-unit-effort data, the conventional linear models and delta-lognormal linear models were employed for the shared aggregated data of monthly and 1° grid resolution in each region. Broadly, the trend of CPUE was similar to that for the previous stock assessment with some dissimilarity in Region 3. The models were diagnosed by the standard residual plots and influence analyses.

INTRODUCTION

Tuna-RFMOs, including the IOTC, recommended that the joint CPUE of longline fisheries be developed to improve the stock assessments for tropical tunas, and thus the IOTC has conducted collaborative works for several years to produce an abundance index by combining CPUEs data from major longline fleets. An ensemble approach of fishery data from multiple longline fleets has been applied to the tropical and temperate tuna species for their stock assessments (e.g. Hoyle et al. 2018, Hoyle et al. 2019a, 2019b, Kitakado et al. 2021a, 2021b, 2022a).

Following these customary practices used in the IOTC and other RFMOs, we conducted a collaborative study for developing abundance indices for the Indian Ocean bigeye tuna based on Japanese, Korean and Taiwanese longline fisheries data up to 2021 by updating our analyses (Kitakado et al. 2022b) reported in the WPTT24(DP) meeting.

MATERIALS

Data sharing protocol

Under the pandemic circumstance, a data sharing protocol among the three countries adopted for the previous analyses of tropical tunas for IOTC and ICCAT and albacore for IOTC was used with a restriction of data access for reduced resolution of data set (not operational data but some aggregated data over 1° square grid by month by vessel). The data set combined for bigeye tuna CPUE standardization were available with data fields of year and month of operation, location to 1° of latitude and longitude, vessel id, number of hooks, and catch by species in number. We classified the species into albacore (ALB), bigeye (BET), yellowfin (YFT), southern bluefin tuna (SBT), black marlin (BLM), blue marlin (BUM), swordfish (SWO), other billfishes (BIL), sharks (SKX) and others (OTH). The data period from the three mebers are as follows:

Japan: 1979-2021

Korea: 1979-2021

Taiwan: 2005-2021

Vessel ID is available from 1975 for Japanese data, but for the consistency with the previous analysis, we used data from 1979. For Taiwanese data, we used data from 2005 onwards due to data quality problems. As for vessel screening, vessels which have more than or equal to 20 data set (one data set means 1-degree grid by month by year by cluster) were used for standardization of CPUE. Figure 1 shows the definition of regions used in the analysis. Except for R3, the proportion of zero catch tends to be negligible.

METHODS

For clustering analyses to account for the change in target, the data were aggregated by 10-days duration (1st-10th, 11th-20th, and 21st~ for each month) based on the agreement in the data sharing protocol of the trilateral collaborative working group. The number of clusters was determined when the relative improvement of SS within-clusters was less than 10%. See some details shown in Wang et al. (2021). In addition to the clustering approach, data of HBF was used for the target index for the tropical areas.

For standardizing the catch-per-unit-effort data, the conventional linear models and delta-lognormal linear models were employed for data of monthly and 1° grid resolution in each region. Considering relatively small zero-catch proportion, we used the lognormal models except for Region 3. Results based on those models were diagnosed by the standard residual plots and influence analysis.

Log-normal (LN) regression models with a constant adjustment

We used an adjustment factor (here 10% of mean of CPUE) to the CPUE data to employ conventional log-normal distributions as follows:

$$\log(CPUE + c) = Main\,effects + Interactions + Error$$

Potential covariates used in the analysis were shown below:

- Temporal component (year, quarter, year*quarter)
- Spatial component (5° squared longitudinal and latitudinal grid)
- Vessel ID
- Cluster category
- HBF averaged within aggregated data: Shallow (<=7), Medium (8<=HBF<=13) and Deep (14 <= HBF)
- Interactions between the spatial component and quarter

The error terms are assumed to be independently and identically distributed as the normal distribution with mean 0 and standard deviation σ. The constant adjustment factor, *c*, is 10% of the overall mean as has been used in previous analyses.

Delta-lognormal (DL) regression model

A delta-lognormal model was also tested to account for "zero data" statistically as has been used in previous analyses (see e.g. Hoyle et al. 2018). For the first component of "zero" or "non-zero" is expressed as a binomial distribution with a probability of "non-zero" catch as a logistic relationship with some explanatory variables, and the second component for positive catch assumed the same regression structures used in the LN regression models with a constant adjustment. The logarithm of the number of hooks was also used in the delta-component of analysis.

Diagnostics and impacts of covariates (Residual plots, Q-Q plots, influence plots)

The standard residual plots were for the diagnosis for fitting of models to the data and Q-Q plots (only for the positive catch component in DL models). In addition, we used influence plots (Bentley et al. 2012) to interpret the contribution of each covariate to the difference between nominal and standardized temporal effects.

Extracts of abundance indices from models with interactions

Once the model fitting and model evaluation were conducted, the final output of the abundance index is extracted through an exercise of the least square means (so-called LS means) to account for heterogeneity of amount of data over covariate categories (as well as the standardized probability of "non-zero" catches in DL models).

RESULTS

Some comparisons of selected results were shown in Figures 4 and 5. Also, the diagnostics and influence plots were shown in Figure 6. General and specific observations are given below:

- For Regions R1N, R1S, and R2, only the lognormal (LN) model was used. The results with the clustering method for accounting target changes showed relatively slow declines compared to those with the HBF and residual plots also showed slightly better shapes in the model with cluster information, but the trend of CPUEs were broadly similar to that for the previous CPUEs. As was suggested in the previous meetings and the continuation of the approach, results with the HBF could be used in the tropical region.
- For region R3, in addition to the LN model, a delta lognormal (DL) model was also applied. Although these results are similar, some difference was observed around 2000 between the previous and new estimates.
- Overall, while not a perfect match, the std-CPUE series selected for this paper shows a generally similar pattern to the CPUE used previously in the 2019 assessment except for R3, as shown in the superimposed figures in Figure 5.
- The current use of aggregated data means that if there is at least one operation in each data grid (1° grid resolution) for each month of each year in each cluster, all three fisheries' data from three fisheries will be equally weighted in the likelihood. However, the degree of information may vary depending on the actual number of operations. This is one of the disadvantages in analysis with aggregated data.
- The results obtained for R1N show a large spike around 2010, which may be due to piracy effects, but cannot be successfully removed in this analysis. In the stock assessment this year, care must be taken in handling this data as in the previous stock assessment.

REFERENCES

Bentley, N., Kendrick, T.H., Starr. P.J. and Breen P.A. 2012. Influence plots and metrics: tools for better understanding fisheries catch-per-unit-effort standardizations. ICES J. Mar. Sci. 69(1): 84-88.

Hoyle, S.D., Chang, S.T., Fu. D., Kim, D.N., Lee, S.I., Matsumoto, T., Chassot, E. and Yeh, Y.M. 2019a. Collaborative study of bigeye and yellowfin tuna CPUE from multiple Indian Ocean longline fleets in 2019, with consideration of discarding. IOTC-2019-WPM10-16.

Hoyle, S.D., Chassot, E., Fu, D., Kim, D.N., Lee, S.I., Matsumoto, T., Satoh, K., Wang, S.P. and Kitakado, T. 2019b. Collaborative study of albacore tuna CPUE from multiple Indian Ocean longline fleets in 2019. IOTC-2019-WPTmT07(DP)-19.

Hoyle, S.D., Kitakado, T., Yeh, Y.M., Wang, S.P., Wu, R.F., Chang, F.C., Matsumoto, T., Satoh, K., Kim, D.N., Lee, S.I., Chassot, E., and Fu, D. 2018. Report of the Fifth IOTC CPUE Workshop on Longline Fisheries, May 28th–June 1st, 2018. IOTC–2018–CPUEWS05–R. 27 pp.

Hoyle, S.D. and Langley, A.D. 2020 Scaling factors for multi-region stock assessments, with an application to Indian Ocean tropical tuans. Fish. Res. 228 https://doi.org/10.1016/j.fishres.2020.105586

IOTC (2018) Report of the Fifth IOTC CPUE Workshop on Longline Fisheries. IOTC-2018-WPM09-INF05.

Kitakado, T., Wang, S.H., Satoh, K., Lee, S.I., Tsai, W.P., Matsumoto, T., Yokoi, H., Okamoto, K., Lee, M.K., Lim, J.H., Kwon, Y., Su, N.J. and Chang, S.T. 2021a. Report of trilateral collaborative study among Japan, Korea and Taiwan for producing joint abundance indices for the yellowfin tunas in the Indian Ocean using longline fisheries data up to 2020. IOTC-2021-WPTT23(DP)-14.

Kitakado, T., Wang, S.H., Satoh, K., Lee, S.I., Tsai, W.P., Matsumoto, T., Yokoi, H., Okamoto, K., Lee, M.K., Lim, J.H., Kwon, Y., Su, N.J. and Chang, S.T. 2021b. Updated report of trilateral collaborative study among Japan, Korea and Taiwan for producing joint abundance indices for the yellowfin tunas in the Indian Ocean using longline fisheries data up to 2020. IOTC-2021-WPTT23(AS)-23.

Kitakado, T., Wang, S.H., Satoh, K., Lee, S.I., Tsai, W.P., Matsumoto, T., Yokoi, H., Okamoto, K., Lee, M.K., Lim, J.H., Kwon, Y., Su, N.J. and Chang, S.T. 2022a. Joint CPUE indices for the albacore Thunnus alalunga in the Indian Ocean based on Japanese, Korean and Taiwanese longline fisheries data. IOTC-2022-WPTmT08(DP)-15.

Kitakado, T., Wang, S.H., Satoh, K., Lee, S.I., Tsai, W.P., Matsumoto, T., Yokoi, H., Okamoto, K., Lee, M.K., Lim, J.H., Kwon, Y., Su, N.J. and Chang, S.T. 2022a. Joint CPUE indices for the albacore Thunnus alalunga in the Indian Ocean based on Japanese, Korean and Taiwanese longline fisheries data. IOTC-2022-WPTT24 (DP)-15.

Matsumoto, T. 2022. Standardization of bigeye CPUE by Japanese longline fishery in the Indian Ocean. IOTC–2022–WPTT24(DP)–14.

Tsai, W.P, Wang, S.H, Wu, H.S and Chang, S.T., 2022. Update on the CPUE standardization of the bigeye tuna caught by the Taiwanese large-scale tuna longline fishery in the Indian Ocean. IOTC-2022-WPTT24-09.

Wang, S.P., Xu, W.Q., Lin, C.Y. and Kitakado, T. 2021. Analysis on fishing strategy for target species for Taiwanese large-scale longline fishery in the Indian Ocean. IOTC-2021-WPB19-11.

Table 1.

		Delta-component						Positive-component				
Model	Distribution	YrQtr	LonLat	Target	Vessel	Ln(Effort)	Interaction	YrQtr	LonLat	Target	Vessel	Interaction
Region 1N	LN							X	X	X (HBF)	X	Qtr:LonLat
Region 1S	LN							X	X	X (HBF)	X	Qtr:LonLat
Region 2	LN							X	X	X (HBF)	X	
Region 3	DL	X	X	X (Clust)		X (offset)		X	X	X (Clust)	X	Qtr:LonLat

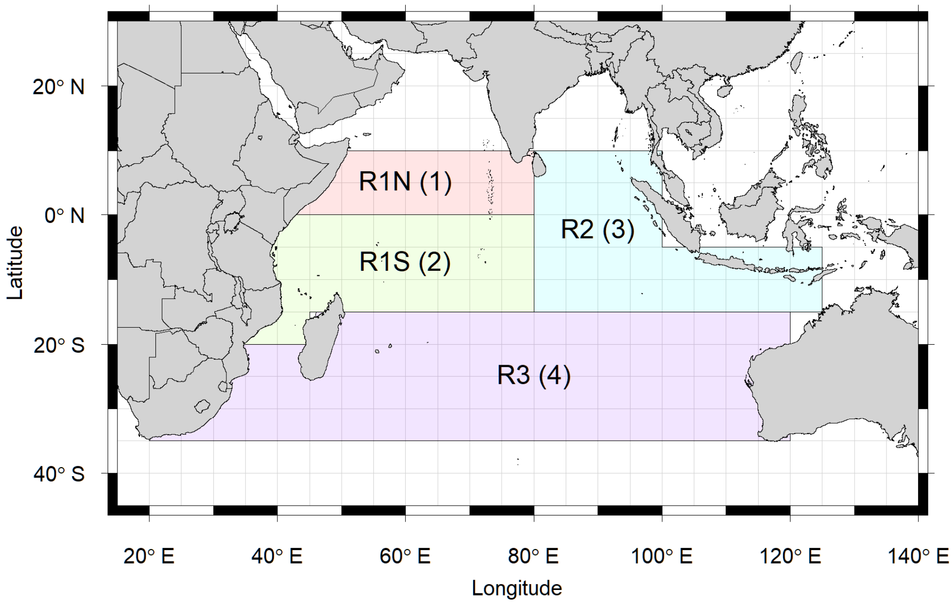

Figure 1. Definition of the regions used in the analysis.

a) Japan

R1N

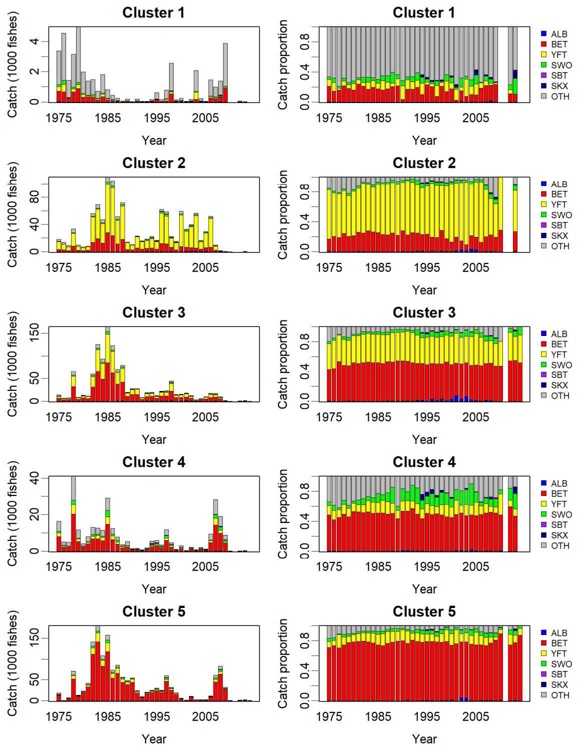

R1S

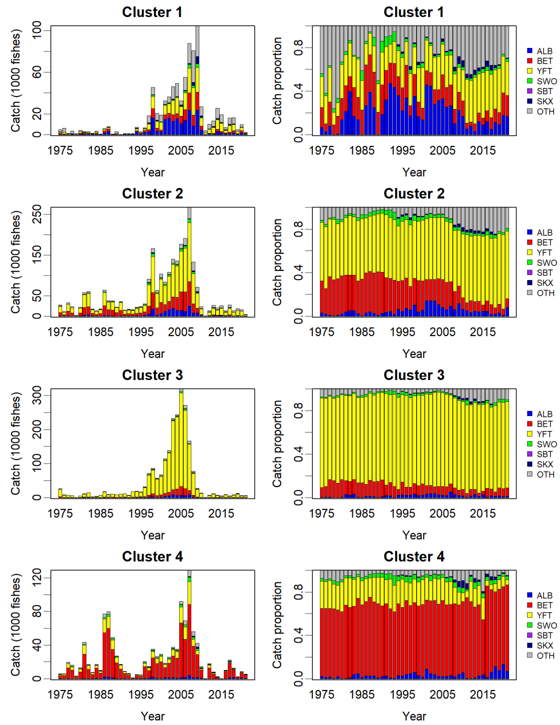

R2

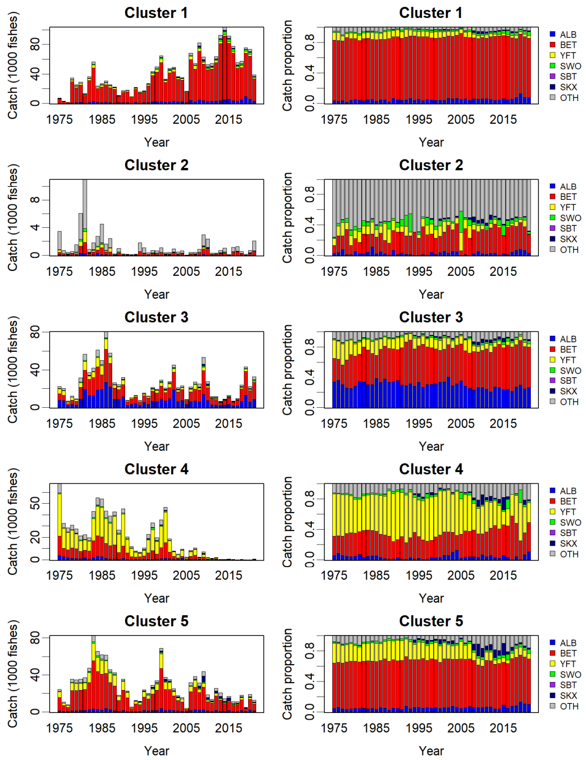

R3

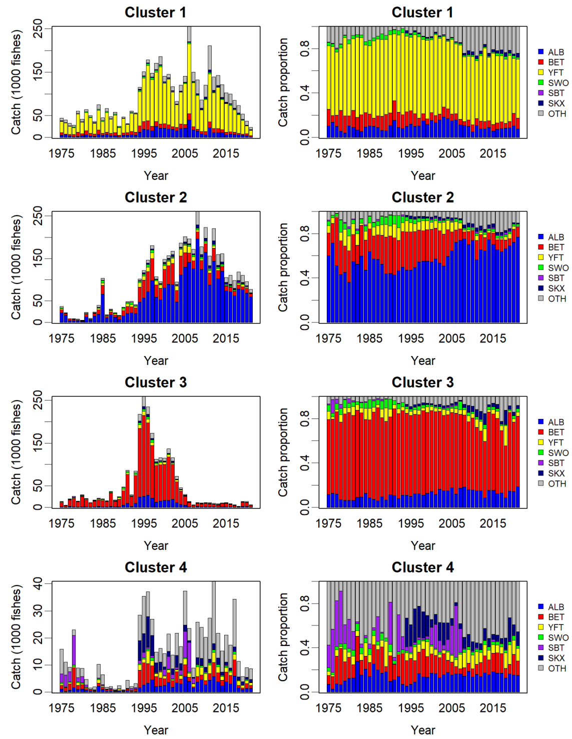

Figure 3(a): Species composition for each cluster in Japanese fisheries.

b) Korea

R1N

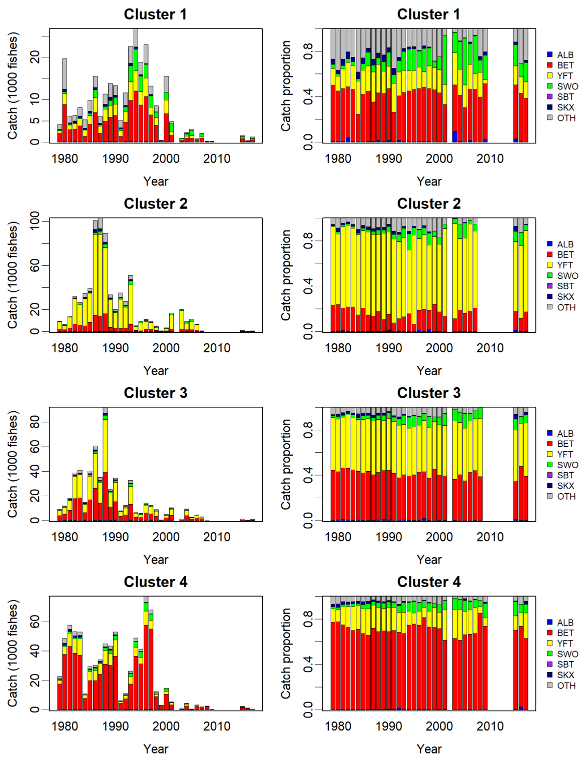

R1S

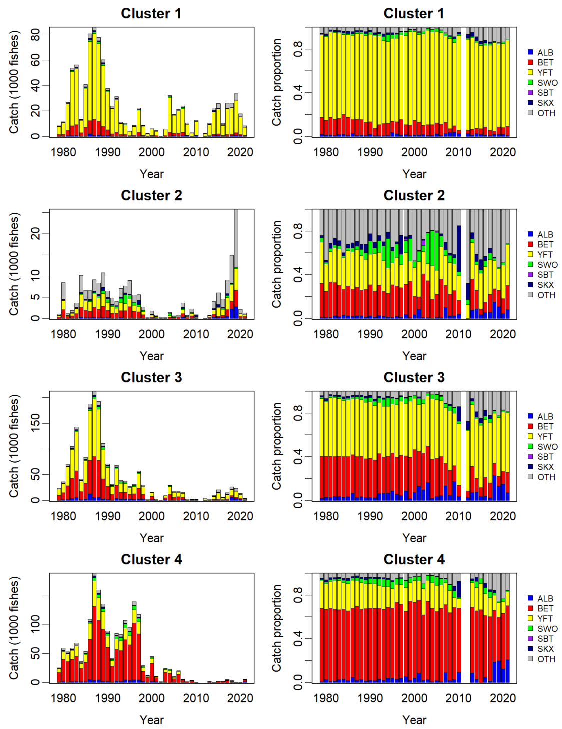

R2

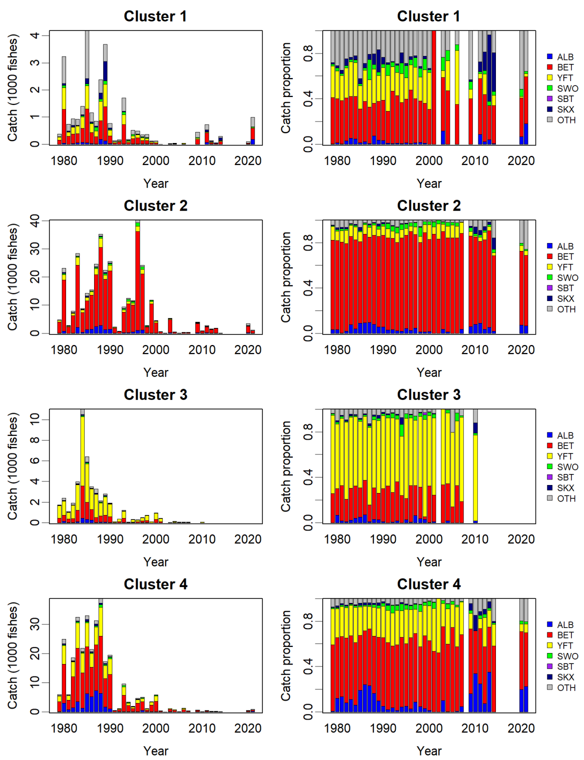

R3

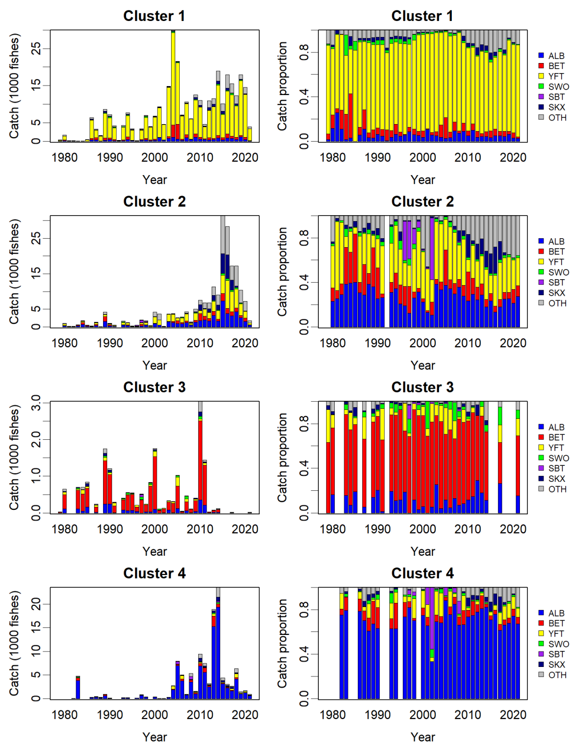

Figure 3(b): Species composition for each cluster in Korean fisheries.

c) Taiwan

R1N

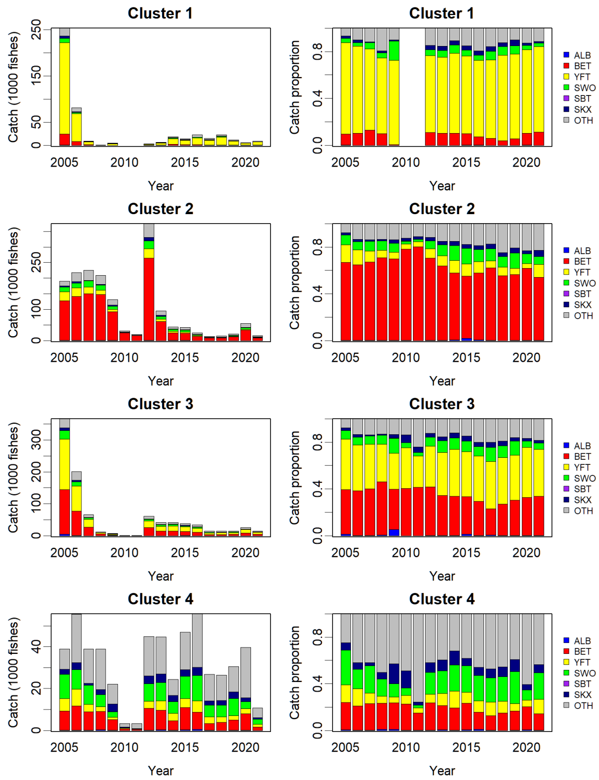

R1S

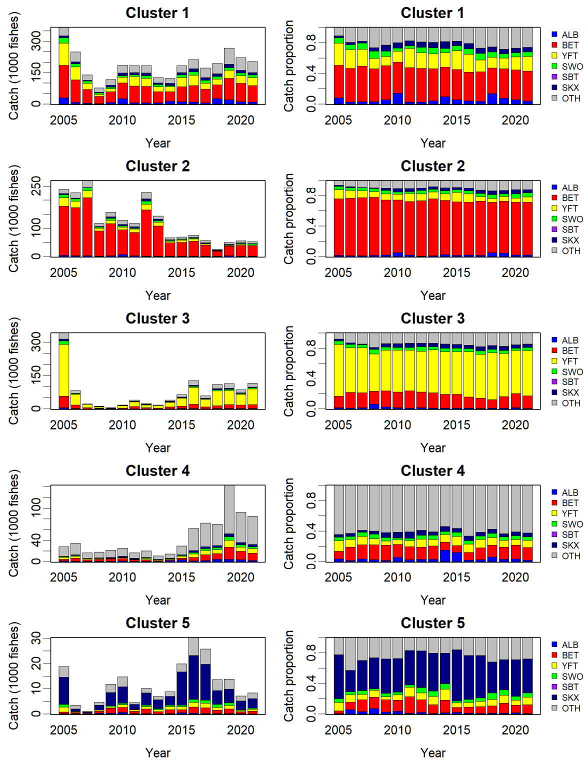

R2

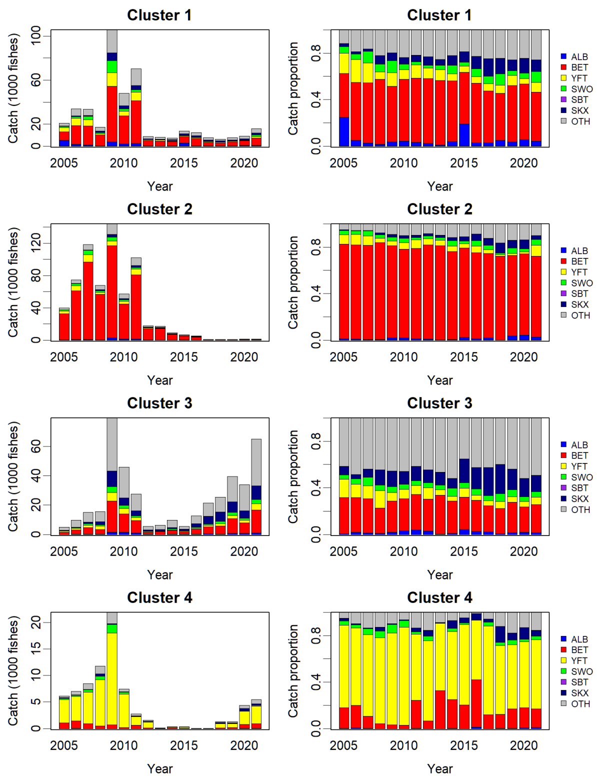

R3

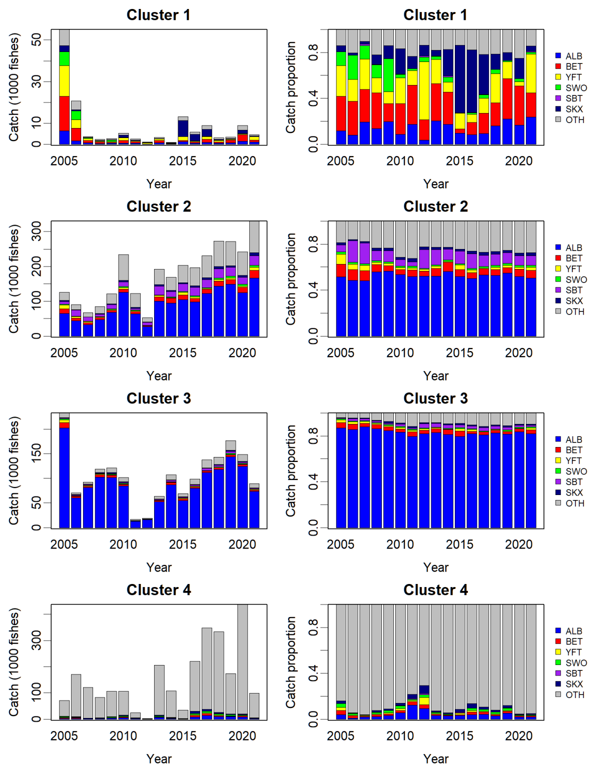

Figure 3(c): Species composition for each cluster in Taiwanese fisheries.

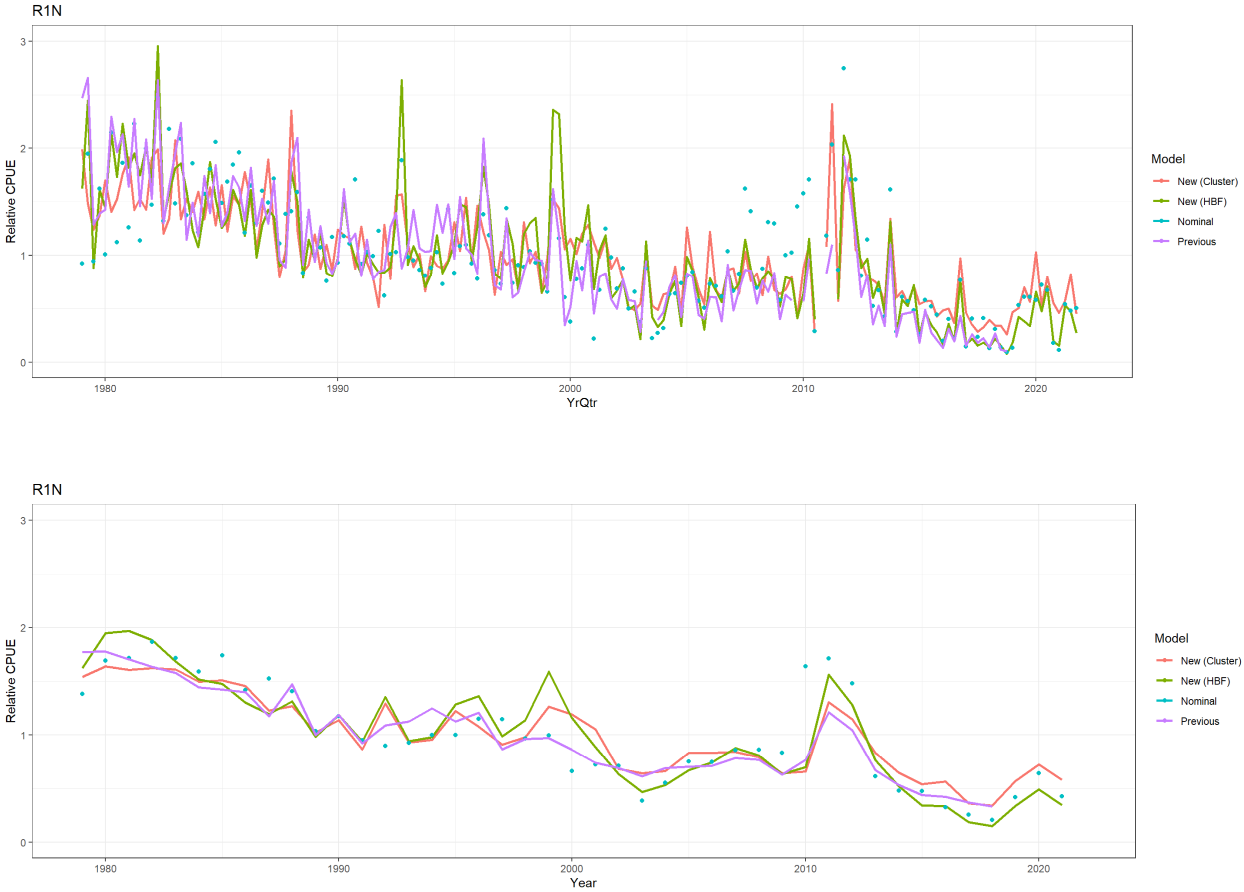

Figure 4(a). Comparison of quarterly (top) and annual (bottom) standardized CPUEs in R1N.

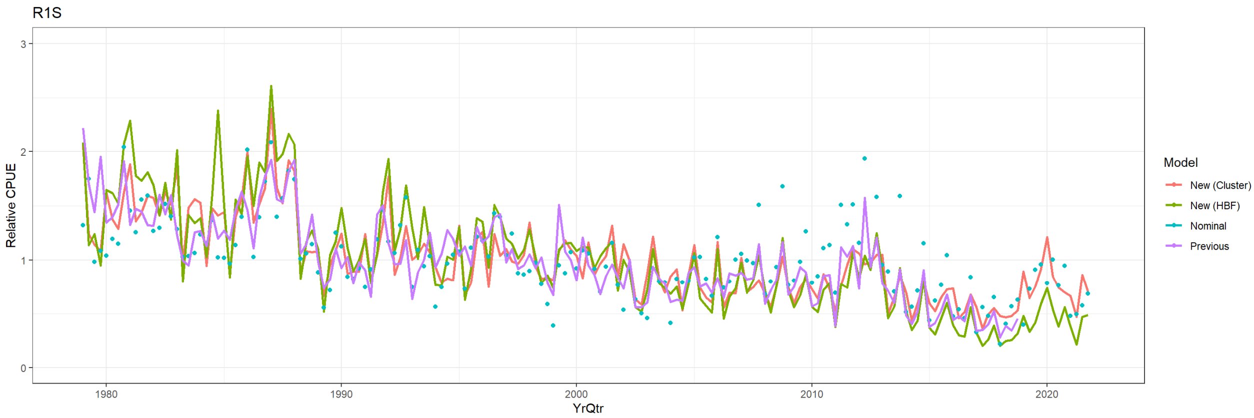

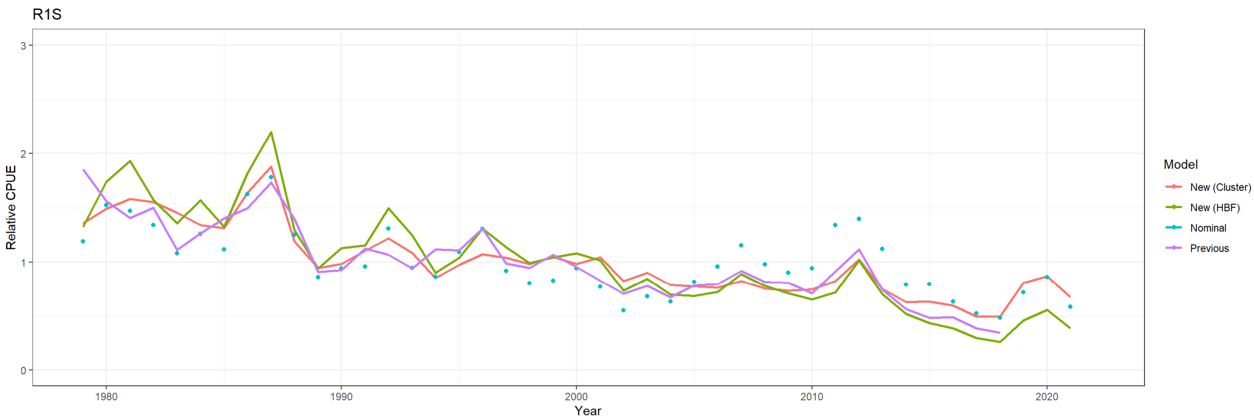

Figure 4(b). Comparison of quarterly (top) and annual (bottom) standardized CPUEs in R1S.

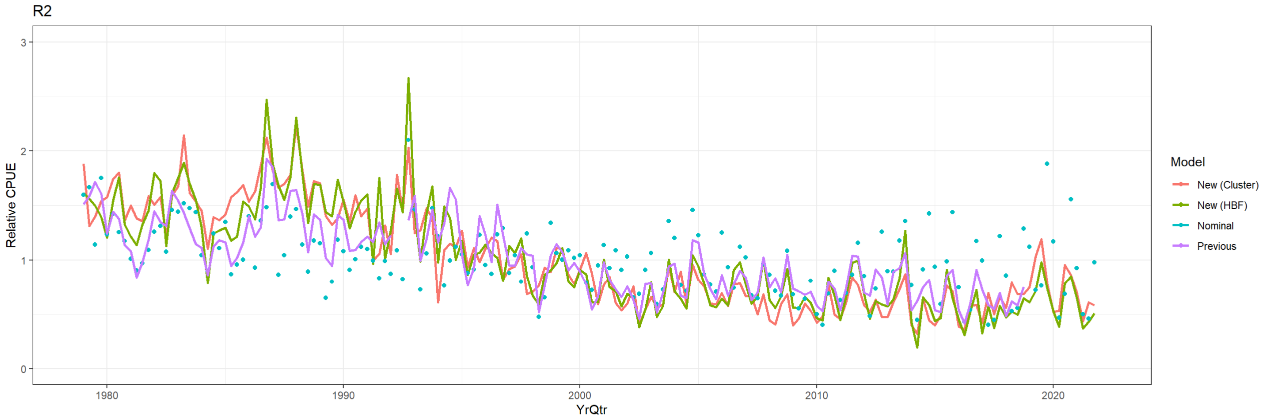

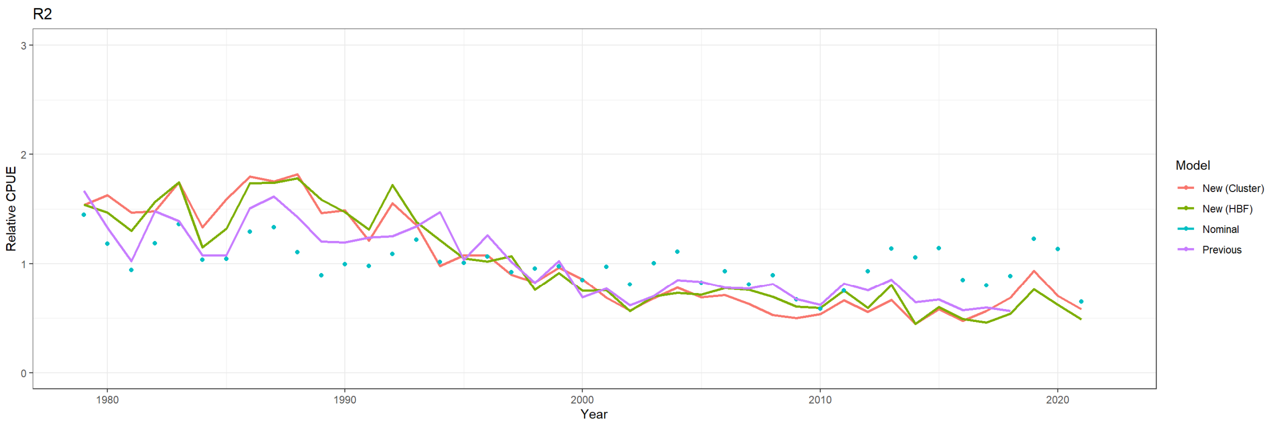

Figure 4(c). Comparison of quarterly (top) and annual (bottom) standardized CPUEs in R2.

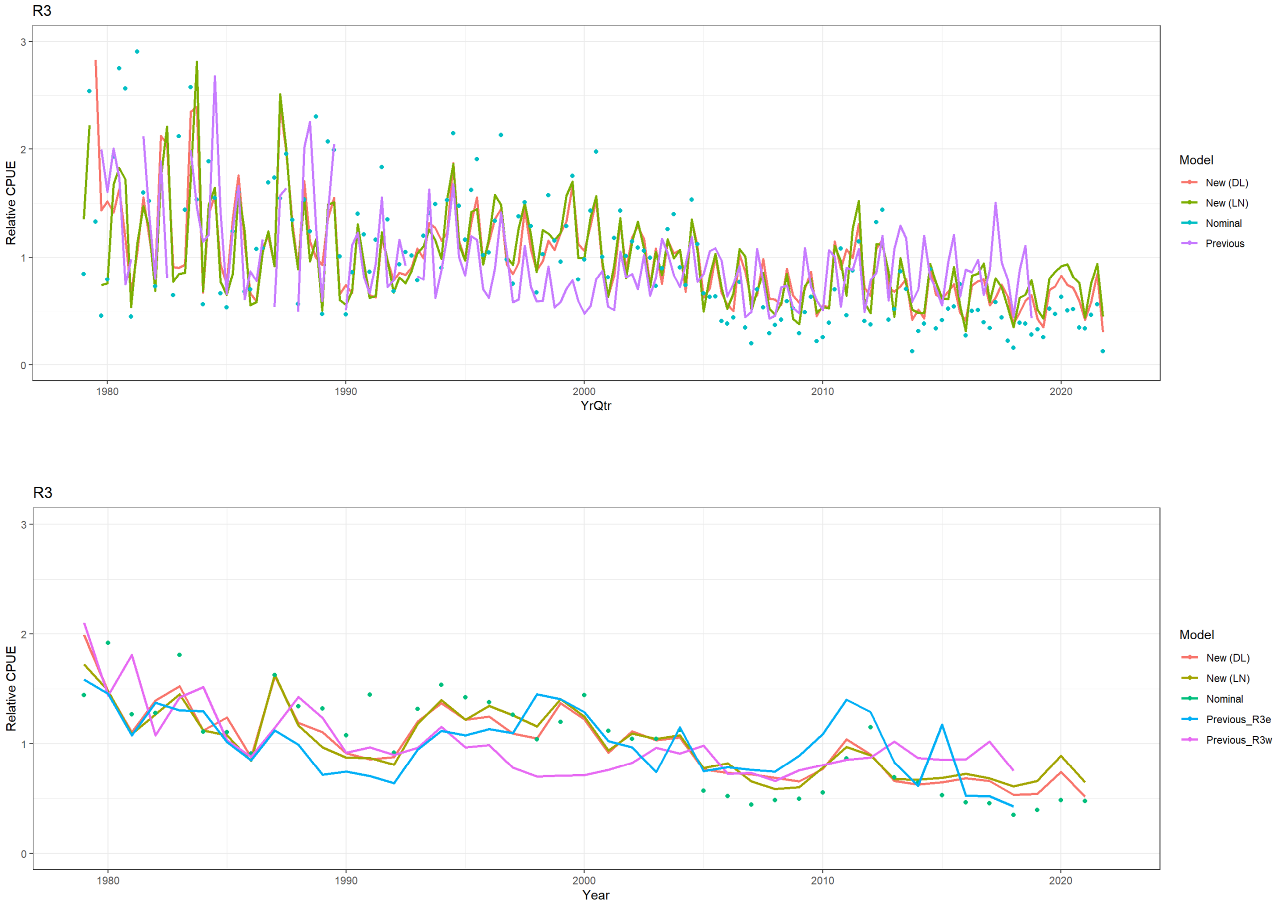

Figure 4(d). Comparison of quarterly (top) and annual (bottom) standardized CPUEs in R3.

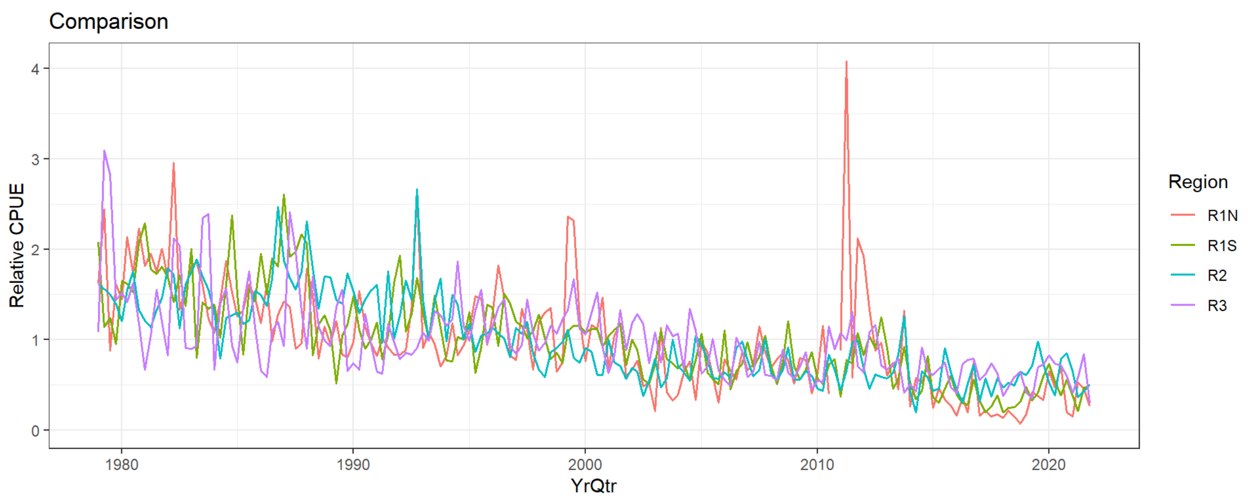

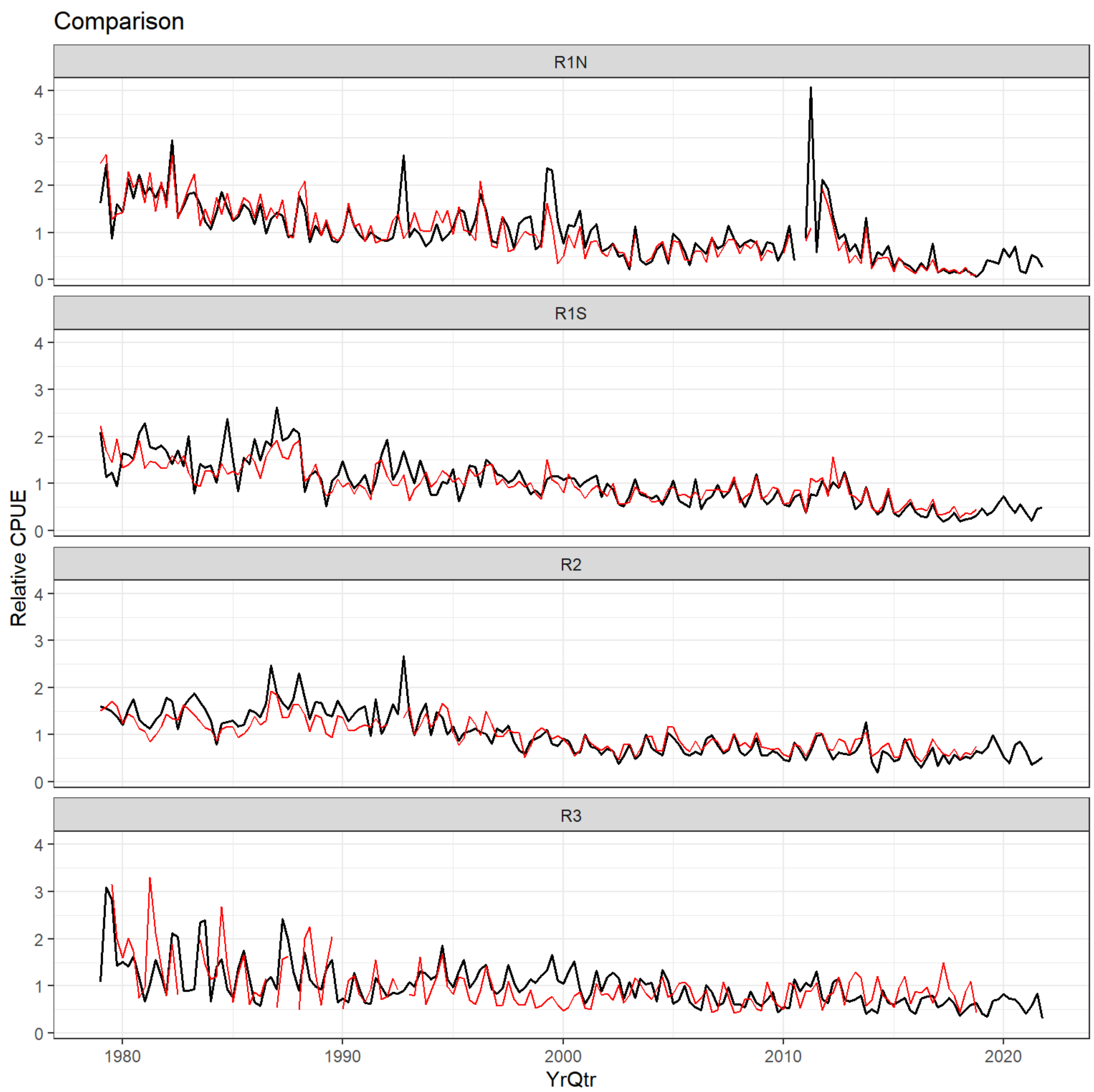

Figure 5(a). Comparison of quarterly region-wise standardized CPUEs (top) and differences between previous (red) and new (black) standardized CPUEs (bottom).

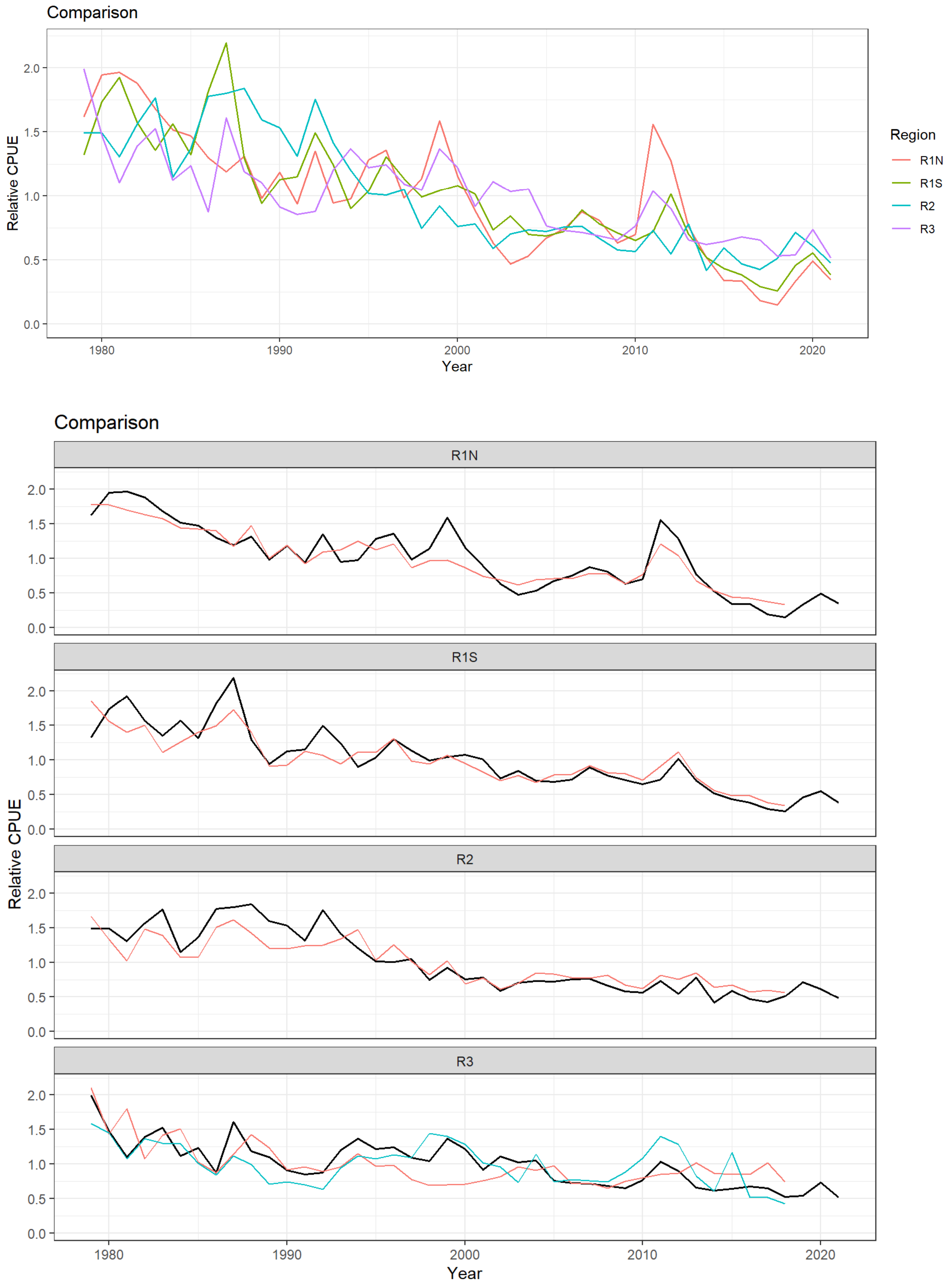

Figure 5(b). Comparison of annual region-wise standardized CPUEs (top) and differences between previous (red or green) and new (black) standardized CPUEs (bottom).

(Cluster model)

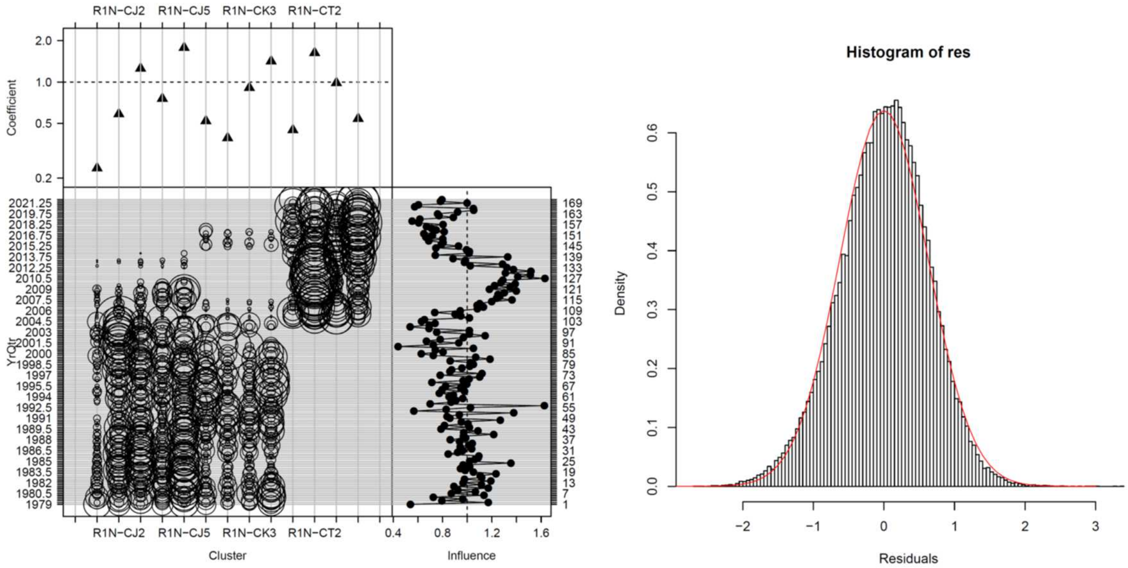

(HBF model)

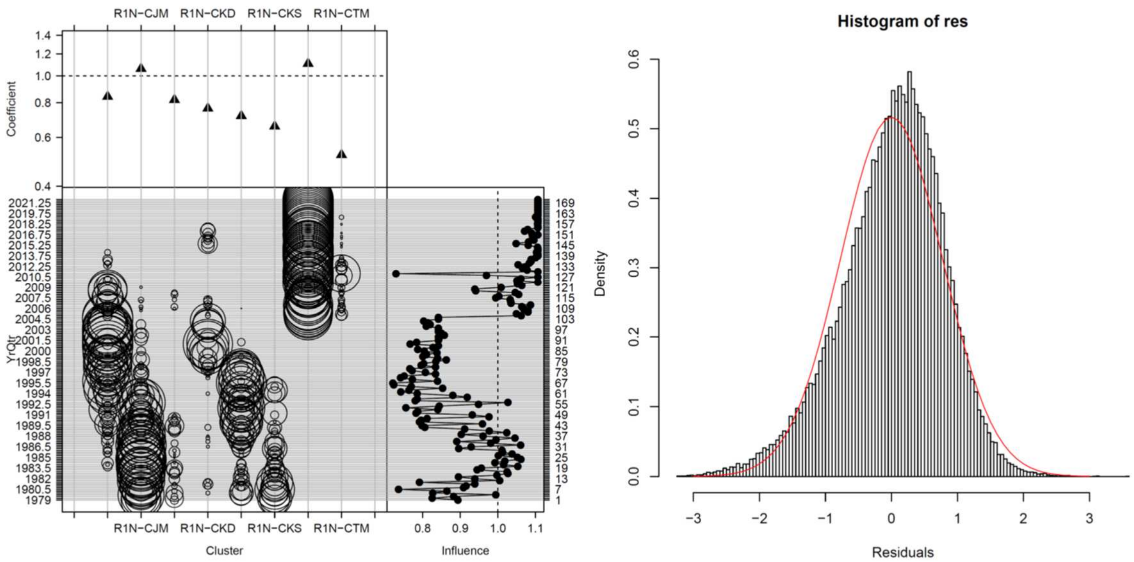

Figure 6(a). Diagnostics and influence plots for the Cluster and Vessel effects for Model LN: YrQ + LonLat + Cluster/HBF + Vessel + LonLat*Q in R1N.

(Cluster model)

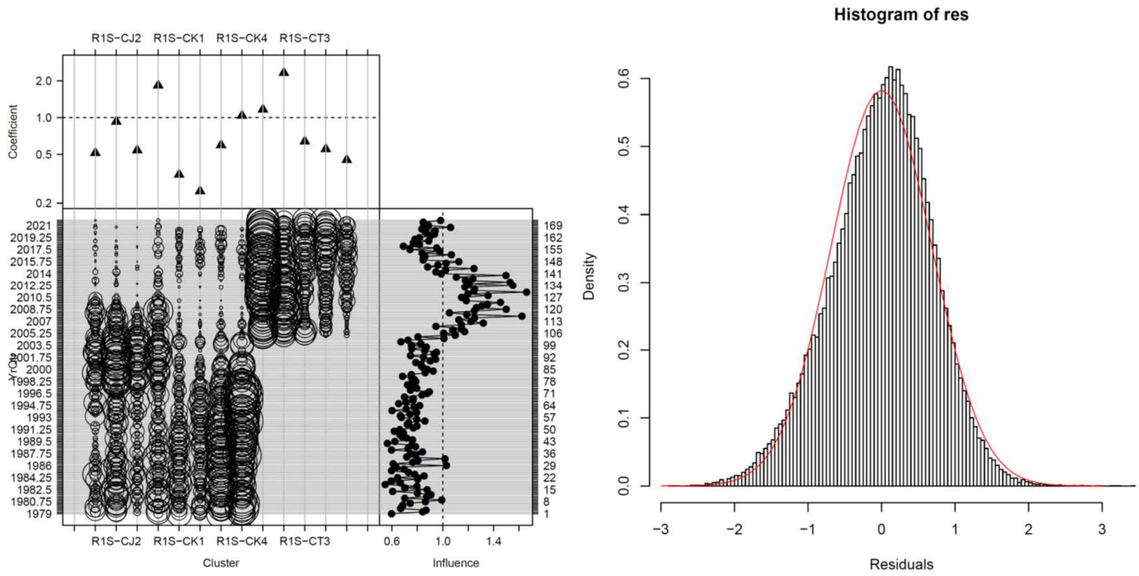

(HBF model)

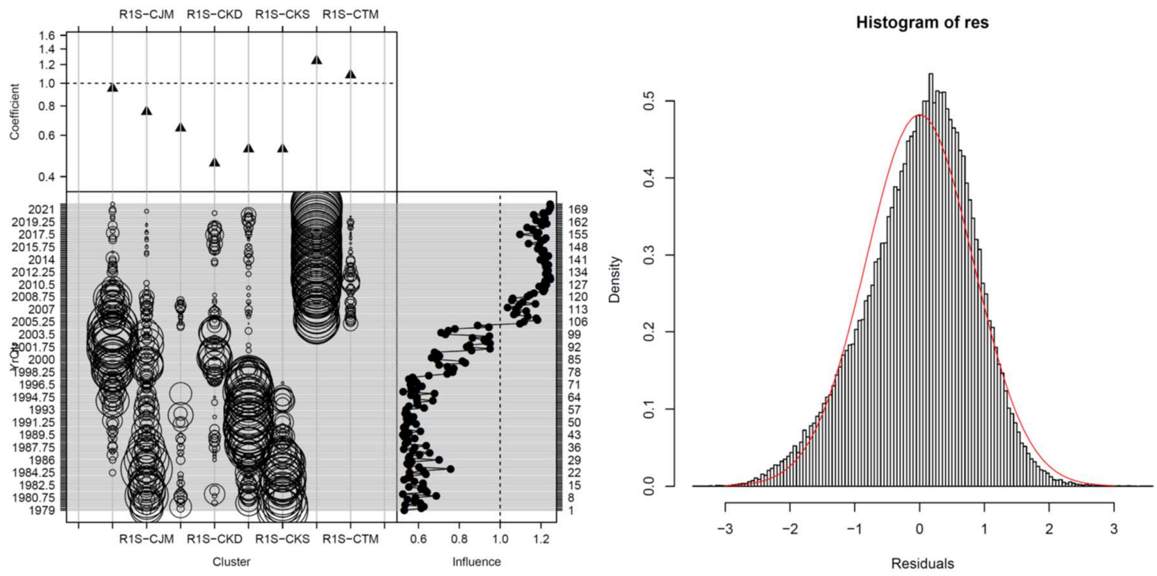

Figure 6(b). Diagnostics and influence plots for the Cluster and Vessel effects for Model LN: YrQ + LonLat + Cluster/HBF + Vessel + LonLat*Q in R1S.

(Cluster model)

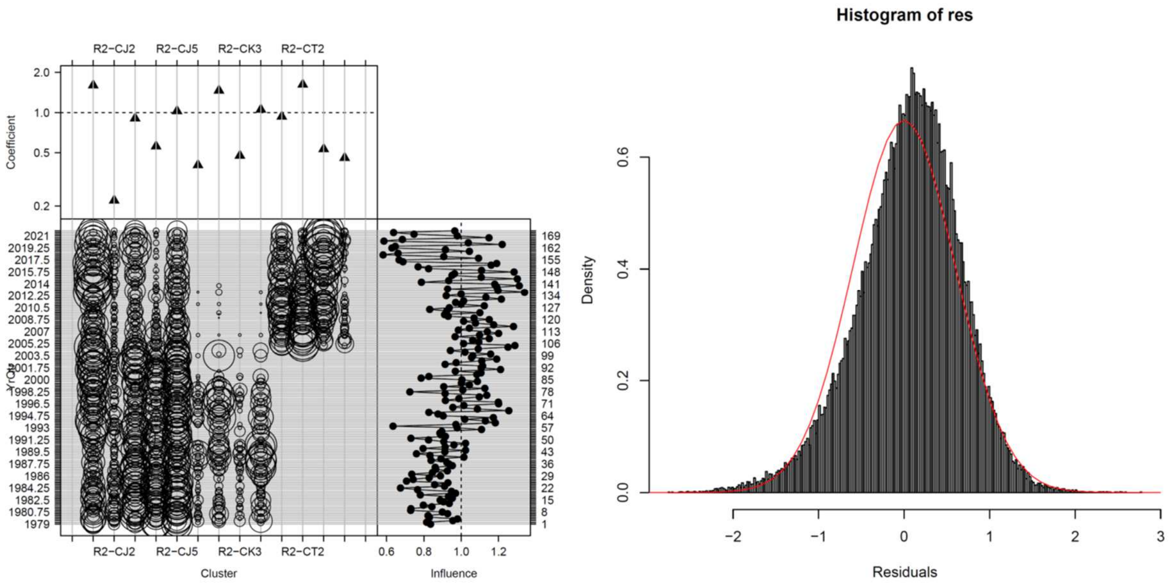

(HBF model)

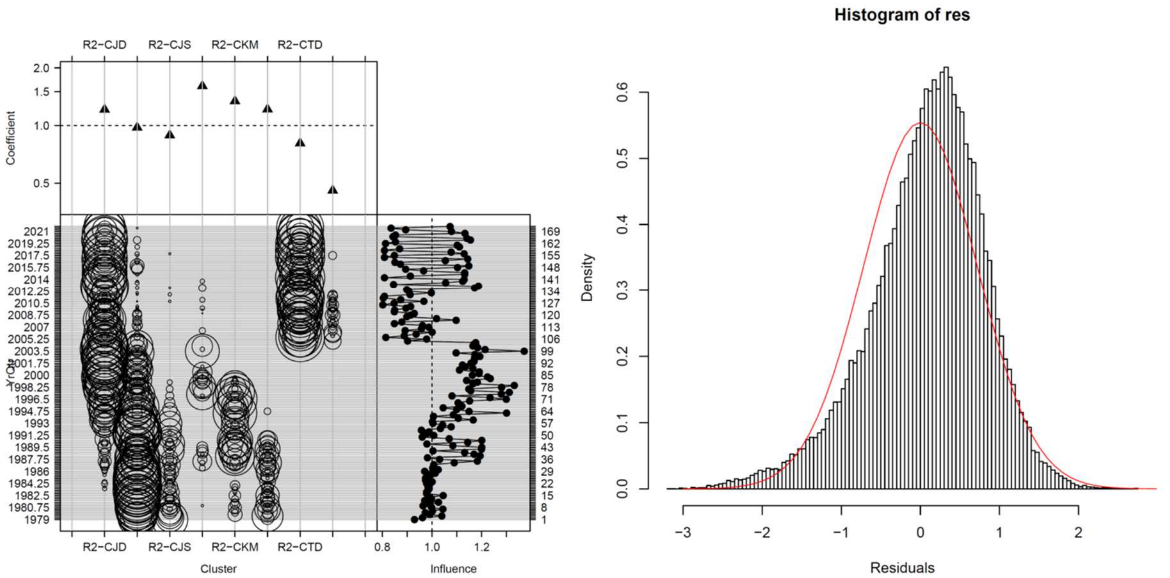

Figure 6(c). Diagnostics and influence plots for the Cluster and Vessel effects for Model LN: YrQ + LonLat + Cluster/HBF + Vessel in R2.

(delta-lognormal model)
[Delta component]

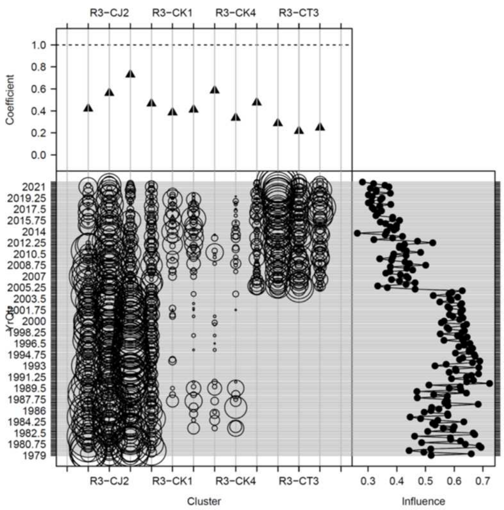

[Positive component]

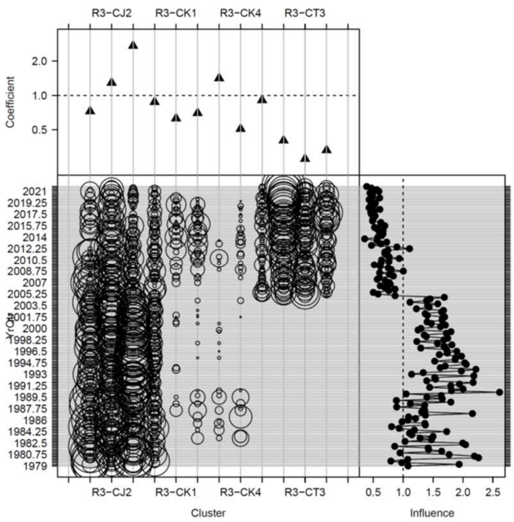

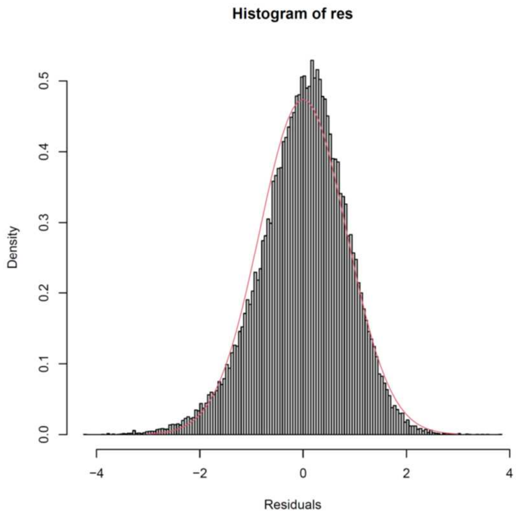

(log-normal model)

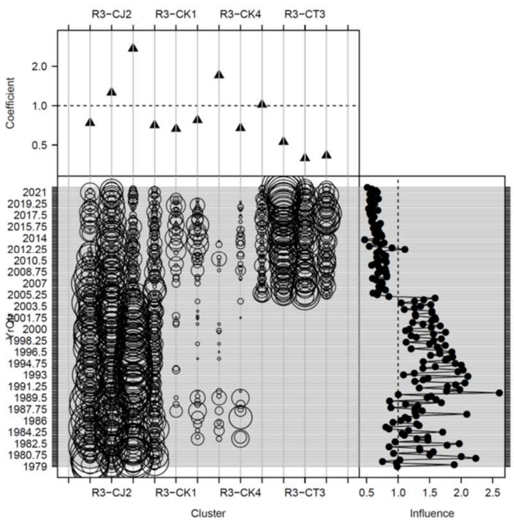

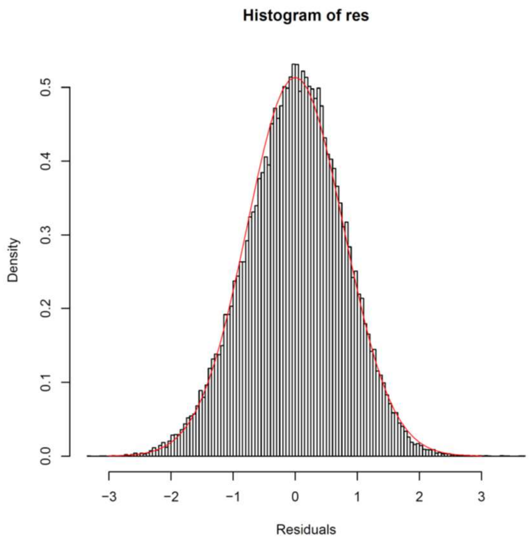

Figure 6(d). Diagnostics and influence plots for delta-lognormal model c1v0e1r0_c1v1r1 (DL: YrQ + LonLat + Cluster + log(Effort), LM: YrQ + LonLat + Cluster +Vessel+ LonLat*Q) in R3.